



20 March 2015 solar eclipse influence on sporadic E layer

M. Pezzopane^{a,*}, M. Pietrella^a, A. Pignalberi^{b,c}, R. Tozzi^a

^a *Istituto Nazionale di Geofisica e Vulcanologia, 00143 Rome, Italy*

^b *Dipartimento di Ingegneria dell'Informazione, Elettronica e Telecomunicazioni, Sapienza Università di Roma, 00185 Rome, Italy*

^c *Istituto per la Scienza dell'Atmosfera e del Clima, CNR, 00133 Rome, Italy*

Received 9 May 2015; received in revised form 10 July 2015; accepted 3 August 2015

Available online 7 August 2015

Abstract

This paper shows how the solar eclipse occurred on 20 March 2015 influenced the sporadic E (Es) layer as recorded by the Advanced Ionospheric Sounder by Istituto Nazionale di Geofisica e Vulcanologia (AIS-INGV) ionosondes installed at Rome (41.8°N, 12.5°E) and Gibilmanna (37.9°N, 14.0°E), Italy. In these locations, the solar eclipse was only partial, with the maximum area of the solar disk obscured by the Moon equal to ~54% at Rome and ~45% at Gibilmanna. Nevertheless, it is shown that the strong thermal gradients that usually accompany a solar eclipse, have significantly influenced the Es phenomenology. Specifically, the solar eclipse did not affect the Es layer in terms of its maximum intensity, which is comparable with that of the previous and next day, but rather in terms of its persistence. In fact, both at Rome and Gibilmanna, contrary to what typically happens in March, the Es layer around the solar eclipse time is always present. On the other hand, this persistence is also confirmed by the application of the height–time–intensity (HTI) technique. A detailed analysis of isoheight ionogram plots suggests that traveling ionospheric disturbances (TIDs) likely caused by gravity wave (GW) propagation have played a significant role in causing the persistence of the Es layer.

© 2015 COSPAR. Published by Elsevier Ltd. All rights reserved.

Keywords: Mid-latitude ionosphere; E sporadic layer; Solar eclipse; Gravity wave; Height–time–intensity technique

1. Introduction

The occurrence of an eclipse generally gives the opportunity of making special observations related to the solar control on the Earth's atmosphere and, in the last decades, it has been well established that the Earth's ionosphere undergoes substantial changes during a solar eclipse event. Specifically, during a solar eclipse, the moon rapidly shadows the Sun and the photochemical activity in the ionosphere decreases almost to nighttime levels. Typically, the ionospheric response is manifested as a decrease of the total electron content (Salah et al., 1986; Afraimovich et al., 1998; Baran et al., 2003; Krankowski et al., 2008; Jakowski et al., 2008), an instantaneous decrease of the

critical frequencies of the E and F1 layers (Adeniyi et al., 2007), and a delayed decrease of the critical frequency of the F2 layer (Cheng et al., 1992; Adeniyi et al., 2007). Another physical phenomenon related to solar eclipses is an enhancement of acoustic gravity waves (AGWs) detected at ionospheric heights (Šauli et al., 2006, 2007).

Many studies were also focused on the eclipse-induced gravity waves (GWs) (Fritts and Luo, 1993; Altadill et al., 2001, 2004; Zerefos et al., 2007; Gerasopoulos et al., 2008), that can be retained responsible for most of the ionospheric eclipse-related phenomena. With regard to this issue, Chimonas and Hines (1971) were the first who suggested that the supersonic speed of the lunar shadow could disturb the thermal balance of the atmosphere and generate gravity waves.

A smaller number of papers are about the solar eclipse effect on sporadic E (Es) layer and the corresponding

* Corresponding author.

E-mail address: michael.pezzopane@ingv.it (M. Pezzopane).

results are conflicting. A decrease of the top frequency of Es (ftEs) was observed by Minnis (1955) and Stoffregen (1955), while an increase was reported by Datta (1973) and Chen et al. (2010). Overall, it seems that the decreasing solar radiation characterizing a solar eclipse has a little direct impact on Es, even though the indirect effects of the eclipse, like the thermal gradient and the GWs, cannot be ignored (Chen et al., 2011).

In this study, the ionograms recorded during the solar eclipse occurred on 20 March 2015 by the Advanced Ionospheric Sounder by Istituto Nazionale di Geofisica e Vulcanologia (AIS-INGV) ionosondes (Zuccheretti et al., 2003) installed at Rome (41.8°N, 12.5°E) and Gibilmanna (37.9°N, 14.0°E), Italy, are considered to show how the Es dynamics is clearly influenced by the solar eclipse conditions. The path of totality passed across the North Atlantic and the Arctic Ocean, moving from the northwest Europe to the northeast Europe, and the only populated sites from which the totality could be seen were the Faroe Islands and Svalbard in the northern Europe. Anyway, the shadow of the eclipse was visible in varying degrees all over Europe.

At Rome and Gibilmanna the solar eclipse was only partial, with the maximum area of the solar disk obscured by the Moon equal to ~54% and ~45%, respectively.

Nevertheless, the features characterizing the Es layer the day of the eclipse are significantly different than those usually characterizing the month of March and specifically the previous and next day of solar eclipse.

Our work wants also to be an additional proof of the evidence that GWs are triggered by eclipse conditions. Moreover, thanks to both the application of the height–time–intensity (HTI) technique proposed by Haldoupis et al. (2006) and the analysis of isoheight ionogram plots, the paper aims at highlighting, that the solar eclipse induced GWs have likely played a significant role in causing the persistence of the Es layer through the wind-shear mechanism.

The analyses and the results are described in detail in Section 2. The discussion of the results and the conclusions are the subject of Section 3.

2. Analysis and results

The ionograms used in this study were those recorded at Rome and Gibilmanna on 19–21 March 2015 by the AIS-INGV ionosondes.

The sweeping frequency range and the sounding repetition rate were respectively set up from 1 MHz to 16 MHz and to 15 min at both stations. From each ionogram the ftEs expressed in MHz was manually validated through the graphical user interface of the software *Interpre* (Pezzopane, 2004). It was decided to refer to ftEs and not to the maximum frequency (foEs) of the Es ordinary mode of propagation because the AIS-INGV ionosonde cannot tag the different modes of propagation, that is the extraordinary (X) and the ordinary (O) one, and for most of ionograms it was practically impossible to distinguish between

foEs and the maximum frequency (fxEs) of the Es extraordinary mode. The characteristic ftEs represents an indirect estimate of the maximum electron density of the Es layer, and it is directly associated to the efficiency of the wind-shear theory.

Fig. 1 shows the plots of ftEs validated data recorded at Rome and Gibilmanna on 19–21 March 2015. The most striking feature shown by Fig. 1 is that the Es layer between 02:30 and 10:15 universal time (UT) at Rome, and between 04:00 and 11:00 UT at Gibilmanna, is always present on 20 March 2015, which is a feature not characterizing the previous and next day, and in general each day of the considered month. By taking into account that the start and end times of the partial solar eclipse as recorded at the ground at Rome and Gibilmanna were about 08:30 UT and 10:30 UT, this suggests that the solar eclipse conditions have somehow influenced the Es dynamics.

This is why we decided to apply first the HTI technique, for investigating the Es layer vertical motion and its variability, and then to generate isoheight plots of electron density to look for the possible presence of traveling ionospheric disturbances (TIDs) caused by GW propagation.

An ionogram represents a snapshot of the ionosphere at the time of the sounding, for definite height and frequency ranges. Hence, from a single ionogram it would not be possible to derive the dynamics of the ionospheric layers. On the contrary, the HTI analysis proposed by Haldoupis et al. (2006), and recently used by Pignalberi et al. (2014) and Oikonomou et al. (2014), to investigate how tidal waves influence the Es dynamics, considers a specific frequency range and, by using a series of ionograms, allows the study of the aforementioned dynamics. The output of the HTI analysis is a plot of the intensity of the energy received by the ionosonde, after being reflected by the ionosphere, versus the 24 h of the day, for a definite frequency range, and for the same height range of the ionogram. With regard to this issue, it is worth noting that the HTI technique has been also used in the recent past to analyze the behavior of the Es layer during some solar eclipse events for frequency ranges of 0.1 MHz (Koucká Knížová and Mošna, 2011).

Figs. 2 and 3 show the three HTI plots, one for each of the considered days, calculated for a frequency range between 1 and 5 MHz by considering the ionograms recorded respectively at Rome and Gibilmanna. This means that each of the plots shown in Figs 2 and 3 is based on the 96 ionograms recorded at Rome and Gibilmanna during each of the three considered days. The maximum of the height range, compared to that of the ionogram, is restricted for simplicity to 210 km. Indeed, the interest of this paper is to highlight phenomena associated with Es layers that are characteristic of altitudes lower than 150 km. In order to generate the HTI plots, an upper limit of 5 MHz was chosen because, as it is possible to infer from Fig. 1, during the considered period the ftEs values are never too much higher than 5 MHz. Figs. 2 and 3 show that the HTI plots generated for the 20 March 2015 are

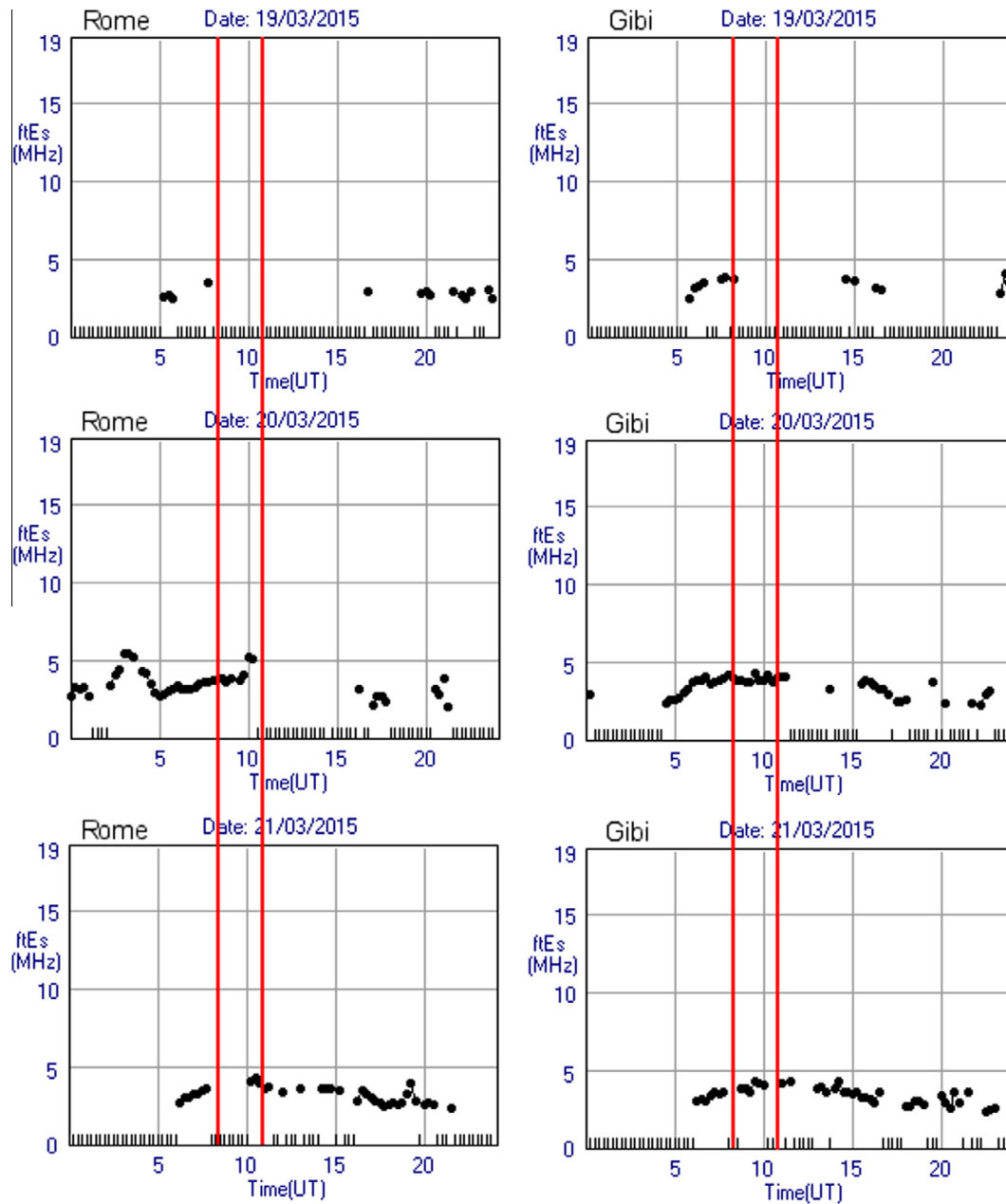


Fig. 1. Plots of ftE_s validated data recorded at (left) Rome and (right) Gibilmanna on 19–21 March 2015. The vertical red lines highlight the start ($\approx 08:30$ UT) and the end ($\approx 10:30$ UT) times of the partial solar eclipse occurred on 20 March 2015, as recorded at the ground. The short black vertical lines at the bottom of each plot mean that the Es layer is not present in the ionogram trace. (For interpretation of the references to color in this figure legend, the reader is referred to the web version of this article.)

characterized by a very distinct Es layer, starting from an altitude of about 125 km at 02:30 UT at Rome and at 04:30 UT at Gibilmanna, and lowering to an altitude of about 100 km where it stops its descent at 12:00 UT at Rome and at 14:00 UT at Gibilmanna. The same pattern is not seen at all in the HTI plots of the previous and next day at both stations. Actually, descent traces seem to be visible also the day after the eclipse but these are fictitious. In fact, at first sight, also these traces could be attributed to the Es layer, but a careful check of the ionograms reveals that this effect is actually caused by the cusp associated

with the electron density maximum of the E region, which is characteristic of the Es layer of type “c” (see also Fig. 2 of Pignalberi et al. (2014)). On the other hand, we are sure that the same artifact does not typify the HTI plot related to the eclipse day because most of the ionograms recorded the 20 March 2015 between 02:00 and 10:00 UT were characterized by blanketing Es layers of type “f” or “i” between 1 and 5 MHz.

In order to look for the possible presence of TIDs caused by gravity wave (GW) propagation, the ionogram traces recorded at Rome and Gibilmanna on 19–21

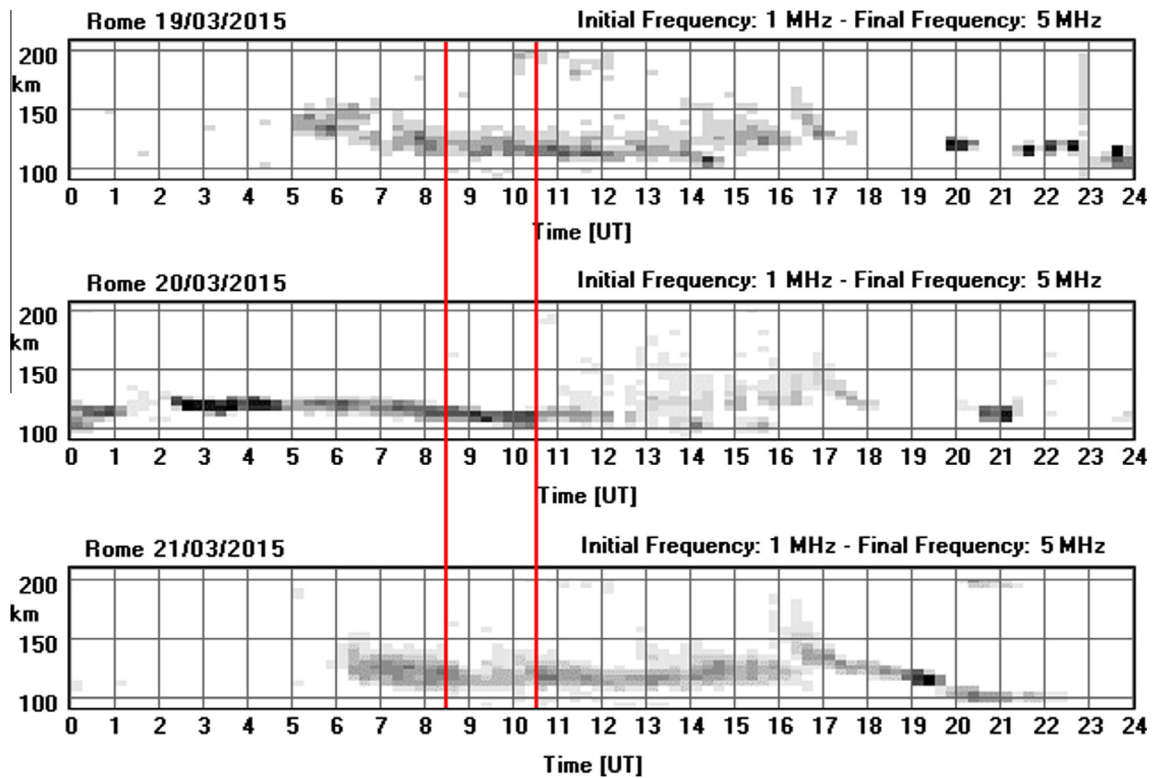


Fig. 2. HTI plots for the 19–21 March 2015, for a frequency range of 1–5 MHz, calculated by considering the ionograms recorded at Rome. The vertical red lines highlight the start ($\approx 08:30$ UT) and the end ($\approx 10:30$ UT) times of the partial solar eclipse occurred on 20 March 2015 as recorded at the ground. (For interpretation of the references to color in this figure legend, the reader is referred to the web version of this article.)

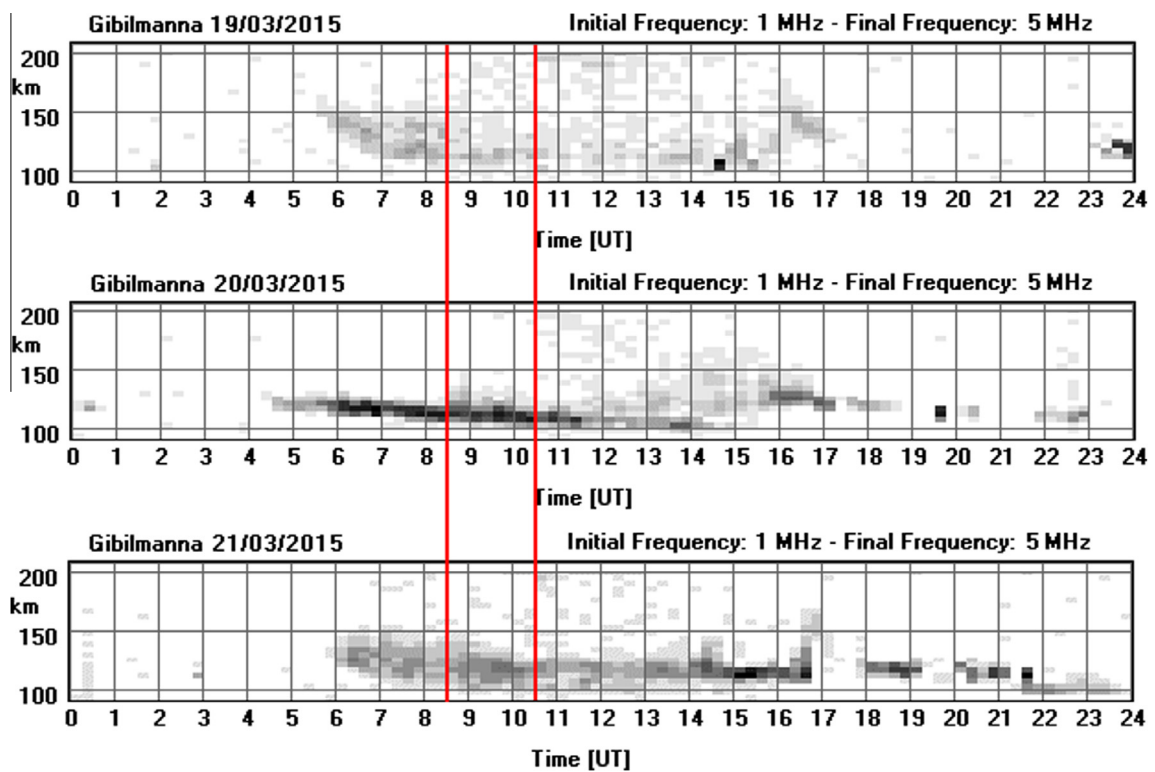


Fig. 3. Same as Fig. 2 for Gibilmanna.

March 2015 from 07:00 to 12:00 UT were manually digitized, obtaining a sequence of couples of values (N , h') for each ionogram, where N is the electron density and h' is the virtual height of reflection. Then, inversion from the ionogram trace (N , h') to the profile (N , h), where h is the real height of reflection, was performed using the POLAN technique (Titheridge, 1988). From the profiles (N , h) isoheight curves ($N(h = \text{const} = 150, 160, 170, 180, 190, 200, 210, 220, 230, 240, 250 \text{ km})$) were then obtained and plotted in Figs 4 and 5 for Rome and Gibilmanna respectively. Both figures show that on 20 March 2015, between 08:00 and 09:00 UT, maximum N variations occur first at higher altitudes and then at lower altitudes, showing a downward phase shift which is characteristic of GW propagation in the ionospheric medium (Hines, 1960). This kind of feature is instead perceivable neither on the 19 March nor on the 21 March 2015.

3. Discussion and conclusions

The mid-latitude ionospheric Es layers, a phenomenon that has been investigated for many years (see reviews by Whitehead, 1989; Mathews, 1998; Haldoupis, 2011, 2012), are thin and dense layers of plasma forming mostly in the region between 90 and 130 km, a region characterized by complicated dynamics and nonlinear plasma processes. The Es layer itself is representative of the complex interaction between the neutral atmosphere and the ionosphere which occurs right in this region.

The ftEs characteristic, associated with the ionic content of the ionospheric E region, presents its maximum values in June and July, which is a well known feature of the mid-latitude Es layer (e.g., Pignalberi et al., 2014; Chu et al., 2014).

The Es occurrence frequency itself shows a behavior which is very similar to that of ftEs; Es layers with lifetimes of 5 h both over Rome and Gibilmanna are observed with the highest percentages of occurrence (80–90%) during summer time (Pietrella et al., 2014).

In fact, in June and July it is not uncommon for the Es layer to be present throughout the day, implying a long persistence of the phenomenon (when talking about persistence we want to stress the fact that we mean a series of consecutive ionograms showing the presence of an Es layer). The same cannot be said for the rest of the months, for which the presence of the Es layer is not absolutely continuous.

Specifically, at the ionospheric stations of Rome and Gibilmanna, in March 2015 there is no day for which the Es layer is continuously present for about 7/8 h; with regard to this issue, the reader can refer to the electronic Space Weather upper atmosphere database (eSWua) (<http://www.eswua.ingv.it/>) (Romano et al., 2008).

The only day that has a persistence of Es layer in the ionogram trace for at least 7/8 h, from about 03 to 11 UT at Rome and from about 04 to 11 UT at

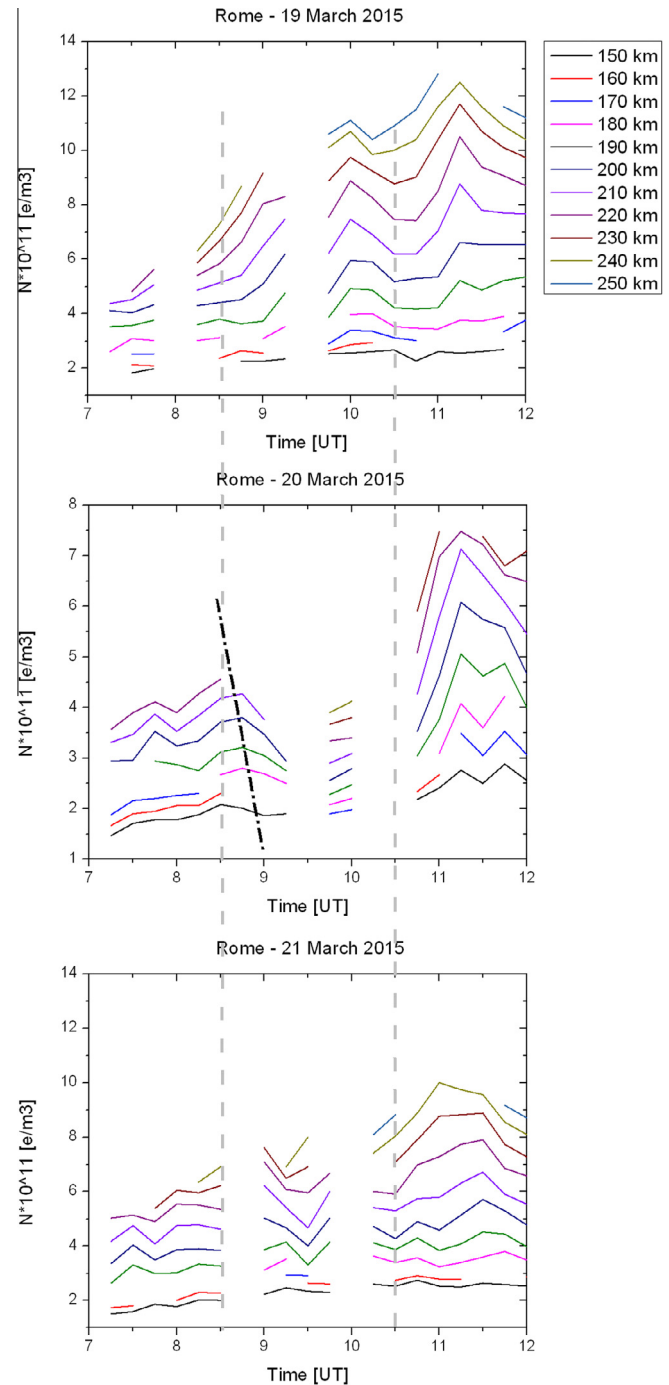


Fig. 4. Electron density variations for the real height range 150–250 km computed for the 19–21 March 2015 from 07 to 12 UT, by considering the ionogram traces recorded at Rome. The oblique line in the middle plot highlights the downward phase shift typical of gravity wave propagation, characterizing the 20 March 2015. The vertical dashed lines highlight the start ($\approx 08:30$ UT) and the end ($\approx 10:30$ UT) times of the partial solar eclipse occurred on 20 March 2015 as recorded at the ground.

Gibilmanna, is the eclipse day (Fig. 1). Both periods of time include the duration time of the partial solar eclipse as recorded at the ground at Rome and Gibilmanna, suggesting as a consequence that the solar eclipse conditions have in some way influenced the Es dynamics.

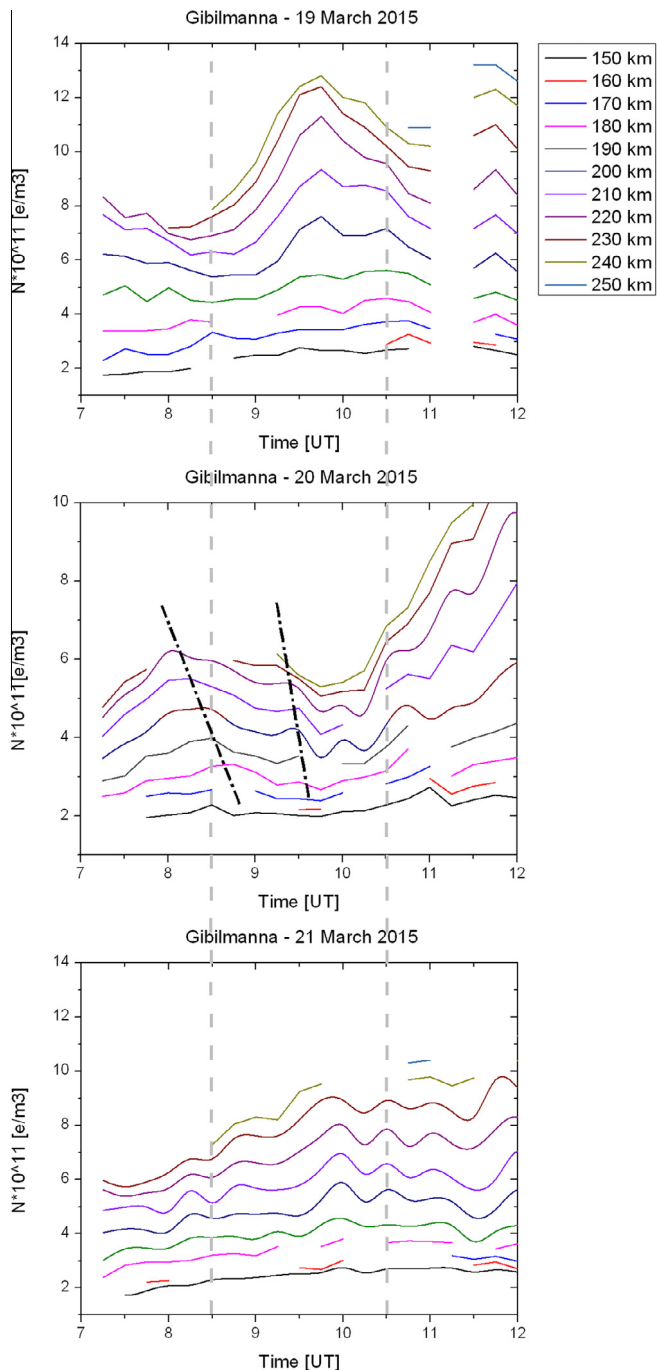


Fig. 5. Same as Fig. 4 for Gibilmanna.

In particular, the solar eclipse did not affect at all the Es layer in terms of its maximum intensity, as it was already reported by other authors (e.g. Datta, 1973; Chen et al., 2010); in fact, the fE_s values do not show any magnitude difference if compared with those of the previous and next day (Fig. 1). This could be due to the fact that the meteoric influx, associated with the ionic content of the ionospheric E region, is in this season, at least in the Northern hemisphere, less than in summer (Haldoupis et al., 2007).

The Es layer is then influenced in terms of its persistence. This persistence is confirmed by the application of the HTI technique proposed by Haldoupis et al. (2006).

Figs. 2 and 3 in fact show that on 20 March 2015, both at Rome and Gibilmanna, in a period of time including that of the solar eclipse, a very distinct Es layer starts at an altitude of about 125 km and lowers to an altitude of about 100 km where it stops its descent; on the contrary, the same pattern does not characterize the previous and next day.

It is believed that the formation of the Es layer relies on vertical wind shears in the neutral horizontal winds, which can force, along with the combined action of ion-neutral collisional coupling and geomagnetic Lorentz forcing, the metallic ions of meteoric origin to move vertically and converge into dense and thin plasma layers localized at the convergence node of the neutral horizontal wind vertical profile.

This Es triggering mechanism was formulated in the early sixties studies mostly associated with the atmospheric gravity waves (Axford, 1963; Chimonas and Axford, 1968).

In Hines and Chimonas (1970) and in Chimonas (1970), it has been shown that, during a solar eclipse, the Moon's cool shadow going through the atmosphere can act as a continuous source of internal gravity waves while running at supersonic speeds across the Earth. Moreover, theoretical considerations on the magnitudes of the pressure perturbations generated from these waves are found to be sufficient to develop TIDs in the ionospheric region that, through the wind-shear mechanism, can cause the appearance of an Es layer.

In the light of these considerations the clear and persistent descending traces visible in Figs 2 and 3 on 20 March 2015 are associated right with a persistent descending convergence node that characterizes the neutral wind profile.

The HTI analysis shows however that persistent Es layers become visible in Rome at 02:30 UT and in Gibilmanna at 04:30 UT, that is at times earlier than those characterizing the eclipse period (08:30–10:30 UT), so that one could also think that the Es persistence is not affected by the eclipse phenomenology. Nevertheless, the wind-shear mechanism causing a persistent descending convergence node, is in all likelihood due to a GW propagation in the ionospheric medium (Hines, 1960), is clearly visible on 20 March 2015 both at Rome and Gibilmanna, between 08:00 and 09:00 UT, that is a time interval included in that of the partial solar eclipse as recorded at the ground. In addition, a careful inspection of Fig. 5 points out another downward phase shift around 09:30 UT, thus indicating the presence of a GW wave train over Gibilmanna. The same cannot be said for Rome, because some ionograms were characterized by blanketing Es which prevented from observing the upper ionospheric layers.

The considerations made above support the fact that the wind-shear system induced by GWs has most likely contributed to the Es persistence observed during the eclipse, the conditions of which have somehow influenced the Es dynamics.

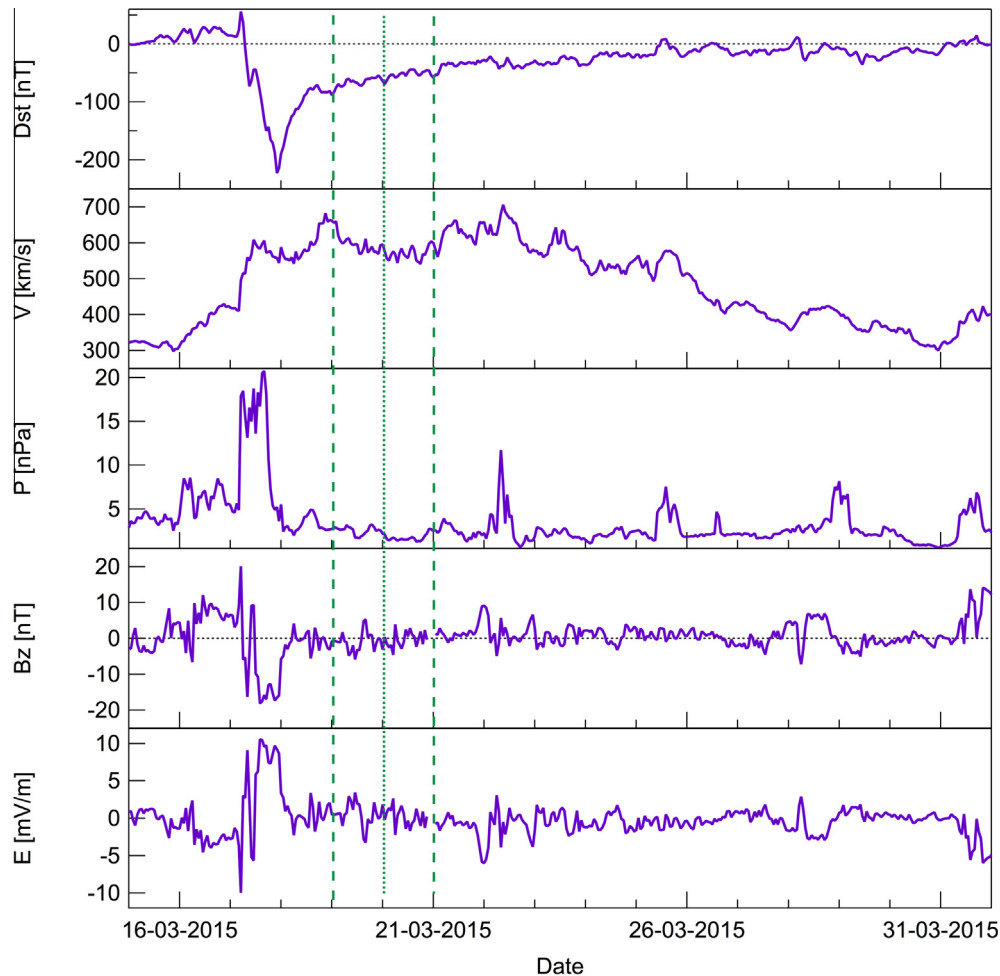


Fig. 6. From top to bottom: Dst index, plasma speed (V), flow pressure (P), interplanetary magnetic field vertical component (B_z) and interplanetary electric field (E) during 15 March–1 April 2015 as contained in the OMNI dataset. Green lines indicate March 20 (dotted) and March 19 and 21 (dashed), respectively. (For interpretation of the references to color in this figure legend, the reader is referred to the web version of this article.)

This is even more convincing if you observe that in the isoheight curves calculated for the previous and next day of the eclipse the downward phase shift is not visible at all.

This is why we think that the uninterrupted presence of a persistent Es layer for 7/8 h observed on 20 March 2015 in the ionogram traces was caused mainly by the strong thermal gradient related to the solar eclipse, which triggered an internal GW, which in turn caused a stable wind-shear mechanism.

Nonetheless, although it is now widely agreed that Es formation at middle latitudes is justifiable according to the wind-shear mechanism, from some numerical simulations related to Es layers observed during the Aladdin 1 rocket campaign, it has emerged that the inclusion of an ad hoc small constant electric field at times can be important to mitigate the discrepancies between modeled and experimental results (MacLeod et al., 1975). Specifically, the effects of the ionospheric ambient electric field have been proved important in producing a persistent Es layer which otherwise by wind effects alone would be rapidly dispersed by diffusion (Rees et al., 1976). With regard to this

issue, it is noteworthy to highlight that the solar eclipse occurred right in the recovery phase of the geomagnetic storm known as St. Patrick's Day geomagnetic storm. This storm commenced on March 17, 2015 with the arrival at Earth of a coronal mass ejection. As can be observed by Fig. 6, the Dst index reached a minimum value of about -200 nT that, together with a Kp index equal to 8, makes of this event a severe magnetic storm.

Even if the mechanism is still not well understood, it is known that the interplanetary electric field can penetrate to the low- and mid-latitude ionosphere due to the interaction among the solar wind, magnetosphere, and ionosphere. Under perturbed geomagnetic conditions this phenomenon can substantially alter the plasma density distribution mainly at low latitudes and mainly during the storm main phase (Wei et al., 2015). So far, little is known on the relation between geomagnetic storms and the Es layer occurrence. Actually, few investigations have been carried out on this relation (e.g. Huang, 1965; Batista and Abdu, 1977; Abdu et al., 2013), all of them focussing on low latitudes, being these latitudes the most significantly

influenced by the penetration electric field, and dealing with the enhancement of Es in terms of electron density rather than on its persistence. However, concerning the case here considered, we can deduce from Fig. 6 that solar wind parameters and interplanetary magnetic field do not exhibit notable differences during the interval 19–21 March. Even if it cannot be excluded that the persistence we observe on March 20 in the Es layer is the effect of the St. Patrick's Day geomagnetic storm, it is not even straightforward to ascribe the observed persistence to either direct or indirect changes in the solar forcing.

In virtue of these considerations, the Es persistence as it has been recorded on 20 March 2015, is more likely to have been triggered by a wave-like activity in terms of GWs caused by thermal gradients related to the solar eclipse, even if we cannot exclude that it could be partly due to the additional electric fields related to the geomagnetically perturbed environment characterizing the period under investigation. A detailed investigation of the latter triggering mechanism is however out of the scope of the present work.

Acknowledgements

We acknowledge use of NASA/GSFC's Space Physics Data Facility's OMNIWeb service, and OMNI data.

References

- Abdu, M.A., Souza, J.R., Batista, I.S., Fejer, B.G., Sobral, J.H.A., 2013. Sporadic E layer development and disruption at low latitudes by prompt penetration electric fields during magnetic storms. *J. Geophys. Res.* 118, 2639–2647. <http://dx.doi.org/10.1002/jgra.50271>.
- Adeniyi, J.O., Radicella, S.M., Adimula, I.A., Willoughby, A.A., Oladipo, O.A., Olawepo, O., 2007. Signature of the 29 March 2006 eclipse on the ionosphere over an equatorial station. *J. Geophys. Res.* 112, A06314. <http://dx.doi.org/10.1029/2006JA012197>.
- Afraimovich, E.L., Palamartchouk, K.S., Perevalova, N.P., Chernukhov, V.V., Lukhnev, A.V., Zalutsky, V.T., 1998. Ionospheric effects of the solar eclipse of March 9, 1997, as deduced from GPS data. *Geophys. Res. Lett.* 25 (4), 465–468. <http://dx.doi.org/10.1029/98GL00186>.
- Altadill, D., Solé, J.G., Apostolov, E., 2001. Vertical structure of a gravity wave like oscillation in the ionosphere generated by the solar eclipse of August 11, 1999. *J. Geophys. Res.* 106 (A10), 21419–21428. <http://dx.doi.org/10.1029/2001JA900069>.
- Altadill, D., Apostolov, E.M., Boska, J., Lastovicka, J., Sauli, P., 2004. Planetary and gravity wave signatures in the F-region ionosphere with impact on radio propagation predictions and variability. *Ann. Geophys.* 47 (2/3). <http://dx.doi.org/10.4401/ag-3288>.
- Axford, W.I., 1963. The formation and vertical movement of dense ionized layers in the ionosphere due to neutral wind shears. *J. Geophys. Res.* 68 (3), 769–779.
- Baran, L.W., Ephishov, I.I., Shagimuratov, I.I., Ivanov, V.P., Lagovsky, A.F., 2003. The response of the ionospheric total electron content to the solar eclipse on August 11, 1999. *Adv. Space Res.* 31 (4), 989–994.
- Batista, I.S., Abdu, M.A., 1977. Magnetic storm associated delayed sporadic E enhancements in the Brazilian geomagnetic anomaly. *J. Geophys. Res.* 82, 4777–4783.
- Chen, G., Zhao, Z., Yang, G., Zhou, C., Yao, M., Li, T., Huang, S., Li, N., 2010. Enhancement and HF Doppler observations of sporadic-E during the solar eclipse of 22 July 2009. *J. Geophys. Res.* 115, A09325. <http://dx.doi.org/10.1029/2010JA015530>.
- Chen, G., Zhao, Z., Zhang, Y., Yang, G., Zhou, C., Huang, S., Li, T., Li, N., Sun, H., 2011. Gravity waves and spread Es observed during the solar eclipse of 22 July 2009. *J. Geophys. Res.* 116, A09314. <http://dx.doi.org/10.1029/2011JA016720>.
- Cheng, K., Huang, Y.-N., Chen, S.-W., 1992. Ionospheric effects of the solar eclipse of September 23, 1987, around the equatorial anomaly crest region. *J. Geophys. Res.* 97 (A1), 103–111. <http://dx.doi.org/10.1029/91JA02409>.
- Chimonas, G., 1970. Internal gravity-wave motions induced in the earth's atmosphere by a solar eclipse. *J. Geophys. Res.* 75 (28), 5545–5551.
- Chimonas, G., Axford, W.I., 1968. Vertical movement of temperate-zone sporadic E layers. *J. Geophys. Res.* 73 (1), 111–117.
- Chimonas, G., Hines, C.O., 1971. Atmospheric gravity waves induced by a solar eclipse, 2. *J. Geophys. Res.* 76 (28), 7003–7005.
- Chu, Y.H., Wang, C.Y., Wu, K.H., Chen, K.T., Tzeng, K.J., Su, C.L., Feng, W., Plane, J.M.C., 2014. Morphology of sporadic E layer retrieved from COSMIC GPS radio occultation measurements: wind shear theory examination. *J. Geophys. Res.* 119, 2117–2136. <http://dx.doi.org/10.1002/2013JA019437>.
- Datta, R.N., 1973. Solar eclipse effect on sporadic E ionization, 2. *J. Geophys. Res.* 78 (1), 320–322.
- Fritts, D.C., Luo, Z., 1993. Gravity wave forcing in the middle atmosphere due to reduced ozone heating during a solar eclipse. *J. Geophys. Res.* 98 (D2), 3011–3021. <http://dx.doi.org/10.1029/92JD02391>.
- Gerasopoulos, E., Zerefos, C.S., Tzagouri, I., Founda, D., Amiridis, V., Bais, A.F., Belehaki, A., Christou, N., Economou, G., Kanakidou, M., Karamanos, A., Petrakis, M., Zanis, P., 2008. The total solar eclipse of March 2006: overview. *Atmos. Chem. Phys.* 8, 5205–5220. <http://dx.doi.org/10.5194/acp-8-5205-2008>.
- Haldoupis, C., 2011. A tutorial review on sporadic E layers, in: *Aeronomy of the earth's atmosphere and ionosphere*, IAGA Special Sopron Book Series 2, 381–394, doi: http://dx.doi.org/10.1007/978-94-007-0326-1_29.
- Haldoupis, C., 2012. Midlatitude sporadic E. A typical paradigm of atmosphere-ionosphere coupling. *Space Sci. Rev.* 168, 441–461. <http://dx.doi.org/10.1007/s11214-011-9786-8>.
- Haldoupis, C., Meek, C., Christakis, N., Pancheva, D., Bourdillon, A., 2006. Ionogram height-time intensity observations of descending E layers at mid-latitude. *J. Atmos. Sol. Terr. Phys.* 68, 539–557. <http://dx.doi.org/10.1016/j.jastp.2005.03.020>.
- Haldoupis, C., Pancheva, D., Singer, W., Meek, C., MacDougall, J., 2007. An explanation for the seasonal dependence of midlatitude sporadic E layers. *J. Geophys. Res.* 112, A06315. <http://dx.doi.org/10.1029/2007JA012322>.
- Hines, C.O., 1960. Internal atmospheric gravity waves at ionospheric heights. *Can. J. Phys.* 38, 1441–1481. <http://dx.doi.org/10.1139/p60-150>.
- Hines, C.O., Chimonas, G., 1970. Atmospheric gravity waves induced by a solar eclipse. *J. Geophys. Res.* 75, 875.
- Huang, Y.N., 1965. Geomagnetic activity and occurrence of sporadic E in far East. *J. Geophys. Res.* 70, 1187–1194.
- Jakowski, N., Stankov, S.M., Wilken, V., Borries, C., Altadill, D., Chum, J., Buresova, D., Boska, J., Sauli, P., Hruska, F., Cander, Lj.R., 2008. Ionospheric behavior over Europe during the solar eclipse of 3 October 2005. *J. Atmos. Solar Terr. Phys.* 70, 836–853.
- Koucká Knížová, P., Mošna, Z., 2011. Acoustic-gravity waves in the ionosphere during solar eclipse events. In: Beghi, Marco G. (Ed.), *Acoustic Waves – From Microdevices to Helioseismology*. InTech. <http://dx.doi.org/10.5772/19722>, ISBN: 978-953-307-572-3, Available from: <<http://www.intechopen.com/books/acoustic-waves-from-microdevices-to-helioseismology/acoustic-gravity-waves-in-the-ionosphere-during-solar-eclipse-events/>>.
- Frankowski, A., Shagimuratov, I.I., Baran, L.W., Yakimova, G.A., 2008. The effect of total solar eclipse of October 3, 2005, on the total electron content over Europe. *Adv. Space Res.* 41, 628–638. <http://dx.doi.org/10.1016/j.asr.2007.11.002>.

- MacLeod, M.A., Keneshea, T.J., Narcisi, R.C., 1975. Numerical modelling of a metallic ion sporadic-E layer. *Radio Sci.* 10 (3), 371–388.
- Mathews, J.D., 1998. Sporadic E: current views and recent progress. *J. Atmos. Sol. Terr. Phys.* 60 (4), 413–435.
- Minnis, C.M., 1955. Ionospheric behaviour at Khartoum during the eclipse of 25th February 1952. *J. Atmos. Terr. Phys.* 6, 91–112.
- Oikonomou, C., Haralambous, H., Haldoupis, C., Meek, C., 2014. Sporadic E tidal variabilities and characteristics observed with the Cyprus Digisonde. *J. Atmos. Sol. Terr. Phys.* 119, 173–183. <http://dx.doi.org/10.1016/j.jastp.2014.07.014>.
- Pezzopane, M., 2004. Interpret: a Windows software for semiautomatic scaling of ionospheric parameters from ionograms. *Comp. Geosci.* 30, 125–130. <http://dx.doi.org/10.1016/j.cageo.2003.09.009>.
- Pietrella, M., Pezzopane, M., Bianchi, C., 2014. A comparative sporadic-E layer study between two mid-latitude ionospheric stations. *Adv. Space Res.* 54 (2), 150–160. <http://dx.doi.org/10.1016/j.asr.2014.03.019>.
- Pignatelli, A., Pezzopane, M., Zuccheretti, E., 2014. Sporadic E layer at mid-latitudes: average properties and influence of atmospheric tides. *Ann. Geophys.* 32, 1427–1440. www.ann-geophys.net/32/1427/2014/.
- Rees, D., Dorling, E.B., Lloyd, K.H., Low, C., 1976. The role of neutral winds and ionospheric electric fields in forming stable sporadic E layers. *Planet. Space Sci.* 24 (5), 475–478.
- Romano, V., Pau, S., Pezzopane, M., Zuccheretti, E., Zolesi, B., De Franceschi, G., Locatelli, S., 2008. The electronic Space Weather upper atmosphere (eSWua) project at INGV: advancements and state of the art. *Ann. Geophys.* 26, 345–351. <http://dx.doi.org/10.5194/angeo-26-345-2008>.
- Salah, J.E., Oliver, W.L., Foster, J.J., Holt, J.M., Emery, B.A., Roble, R.G., 1986. Observation of the May 30, 1984, annular solar eclipse at Millstone Hill. *J. Geophys. Res.* 91 (A2), 1651–1660.
- Šauli, P., Abry, P., Boška, J., Duchayne, L., 2006. Wavelet characterization of ionospheric acoustic and gravity waves occurring during the solar eclipse of August 11, 1999. *J. Atmos. Sol. Terr. Phys.* 68 (3–5), 586–598. <http://dx.doi.org/10.1016/j.jastp.2005.03.024>.
- Šauli, P., Roux, S.G., Abry, P., Boška, J., 2007. Acoustic-gravity waves during solar eclipses: detection and characterization using wavelet transforms. *J. Atmos. Sol. Terr. Phys.* 69 (17–18), 2465–2484. <http://dx.doi.org/10.1016/j.jastp.2007.06.012>.
- Stoffregen, W., 1955. Variation of fEs during solar eclipses. *Nature* 176, 610.
- Titheridge, J.E., 1988. The real height analysis of ionograms: a generalized formulation. *Radio Sci.* 23 (5), 831–849. <http://dx.doi.org/10.1029/RS023i005p00831>.
- Wei, Y., Zhao, B.Q., Li, G.Z., Wan, W.X., 2015. Electric field penetration into Earth's ionosphere: a brief review for 2000–2013. *Sci. Bull.* 60, 748–761. <http://dx.doi.org/10.1007/s11434-015-0749-4>.
- Whitehead, J.D., 1989. Recent work on mid-latitude and equatorial sporadic-E. *J. Atmos. Terr. Phys.* 51 (A5), 401–424.
- Zerefos, C.S., Gerasopoulos, E., Tsagouri, I., Psiloglou, B.E., Belehaki, A., Herekakis, T., Bais, A., Kazadzis, S., Eleftheratos, C., Kalivitis, N., Mihalopoulos, N., 2007. Evidence of gravity waves into the atmosphere during the March 2006 total solar eclipse. *Atmos. Chem. Phys.* 7, 4943–4951. <http://dx.doi.org/10.5194/acp-7-4943-2007>.
- Zuccheretti, E., Tutone, G., Sciacca, U., Bianchi, C., Arokiasamy, B.J., 2003. The new AIS-INGV digital ionosonde. *Ann. Geophys.* 46 (4), 647–659.